

Final Mass and Maximum Spin of Merged Black Holes and the Golden Black Hole

James Healy,¹ Pablo Laguna,² Richard A. Matzner,³ and Deirdre M. Shoemaker²

¹*Center for Gravitational Wave Physics*

The Pennsylvania State University, University Park, PA 16802

²*Center for Relativistic Astrophysics and School of Physics*

Georgia Institute of Technology, Atlanta, GA 30332

³*Center for Relativity and Department of Physics*

The University of Texas at Austin, Austin, TX 78712

We present results on the mass and spin of the final black hole from mergers of equal mass, spinning black holes. The study extends over a broad range of initial orbital configurations, from direct plunges to quasi-circular inspirals to more energetic orbits (generalizations of Newtonian elliptical orbits). It provides a comprehensive search of those configurations that maximize the final spin of the remnant black hole. We estimate that the final spin can reach a maximum spin $a/M_h \approx 0.99 \pm 0.01$ for extremal black hole mergers. In addition, we find that, as one increases the orbital angular momentum from small values, the mergers produce black holes with mass and spin parameters $\{M_h/M, a/M_h\}$ spiraling around the values $\{\widehat{M}_h/M, \widehat{a}/M_h\}$ of a *golden* black hole. Specifically, $(M_h - \widehat{M}_h)/M \propto e^{\pm B \phi} \cos \phi$ and $(a - \widehat{a})/M_h \propto e^{\pm C \phi} \sin \phi$, with ϕ a monotonically growing function of the initial orbital angular momentum. We find that the values of the parameters for the *golden* black hole are those of the final black hole obtained from the merger of a binary with the corresponding spinning black holes in a quasi-circular inspiral.

PACS numbers:

Introduction: An important question that can only be answered with the tools provided by numerical relativity is: What is the final mass and maximum spin of the final black hole (BH) from generic binary mergers? In Ref. [1], referred to here as Paper I, we took the first step towards answering this question. We studied the behavior of a 1-parameter series of equal mass, non-spinning BHs in merger or fly-by. The adjustable parameter was the magnitude of initial linear momentum P for each of the BHs. We kept fixed the initial binary coordinate separation $\vec{d} = 10 M \hat{x}$ and the angle $\theta = 26.565^\circ$ between \vec{P} and \vec{d} . That is, the binaries had initial orbital momentum $\vec{L} = d P \sin \theta \hat{z} = 4.47 M P \hat{z}$ and impact parameter $b = d \sin \theta = 4.47 M$. Here $M = 2m$ is the total mass of the binary, where m is the mass of each BH. The main result in Paper I was the specific dependence or transfer function we found that connects the final merged BH spin a/M_h with the initial L/M_{adm}^2 (see Fig. 1 in Paper I, which is repeated in Fig. 1 here in the curve labeled as $S/M^2 = 0.0$, *i.e.* vanishing total initial spin). For this case, a maximum final BH spin $a/M_h \approx 0.82$ was found at $L/M_{adm}^2 \approx 1$.

The result of Paper I has particular astrophysical interest as an upper limit on the spin from initially non-spinning BH mergers, though BHs can be spun up by other processes as well, specifically by accretion. No previous BH merger simulation has produced final spins close to maximal. We do know from specific examples in work by Campanelli *et al.* [2] that “hangups” occur, in which the orbital radius decreases only slowly or not at all, and which enable the radiation of substantial angular momentum before the merger. In Paper I, we also found a splash-skip behavior involving what Pretorius and Khurana [3] called whirl orbits. In these cases the

interacting BHs can approach, then recede to a large distance, then approach again, producing repeated bursts of gravitational radiation. This is clearly an extreme case of “hangup.”

Here we extend the work in Paper I to encounters where at least one of the BHs carries a spin, with the spins parallel or anti-parallel to the orbital angular momentum. The main motivation is to add extra initial angular momentum in order to increase the final BH spin. In addition, we vary the angle θ , but keep the initial separation as before, $d = 10 M$. We find similar transfer functions to that in Paper I, with the maximum final BH spin depending on the spins of the merging BHs and the scattering angle θ . Our simulations show that the final BH can reach a maximum spin $a/M_h \approx 0.99 \pm 0.01$ when extrapolated to the merger of maximally spinning BHs.

In addition, we found an interesting behavior regarding the parameters $\{M_h/M, a/M_h\}$ of the final BH as we increased the orbital angular momentum. The values for $\{M_h/M, a/M_h\}$ spiral around the parameters of what we operationally call a *golden* BH. We have been able to identify the *golden* BH to be the hole obtained from the merger of a binary in a quasi-circular inspiral with the corresponding spinning BHs.

The computational setup for the simulations presented here is very similar to the one in Paper I, the main difference being the spins of the colliding BHs. All simulations had 10 levels of refinement, sixth order spatial differencing, with an outer boundary of $\sim 320 M$. For the runs used to compute the $\theta \geq 26.565^\circ$ maximum final spin ($\sim 200 - 300 M$ runtimes) a resolution of $M/51.6$ was used on the finest level, with each subsequent level decreased by a factor of 2. For the $\theta < 26.565^\circ$ runs ($\sim 200 - 300 M$ runtimes), a resolution of $M/103$ was

used. For the longer runs to compute the *golden* BH ($\sim 500 - 3000 M$ runtimes), a resolution of $M/90$ was used on the finest grid.

The present study required $\sim 1,000$ binary black holes (BBH) simulations. Every data point displayed in each figure involves at least one BBH simulation and in Figs. 2 and 3 up to ten simulations. It was thus prohibitively expensive to do the runs needed to estimate errors via Richardson extrapolation for each data point. With this in mind, we chose to do all the simulations at the resolutions mentioned in the previous paragraph, which by experience we know our code yields sufficiently accurate results. In order to get error estimates, we selected a subset of representative cases, in some instances the most challenging cases (e.g. high BH spins), to perform convergence tests and apply Richardson extrapolation. Those are the cases with error bars in Figs. 1, 3 and 5. The convergence tests demonstrated consistency with the expected fourth order accuracy of our code. In addition, the Richardson extrapolation of results yielded error bars for the spin and mass of the final black hole $\sim 0.1\%$. For situations involving BH spins $a/M_h \geq 0.95$, we identified additional sources of error due to inaccuracies in finding the exact location of the apparent horizon (AH) that yield errors in the range between 0.5 and 1%.

Maximum Final Black Hole Spin: The first component of this work is aimed at addressing the following three questions regarding the maximum spin of the final BH: Does the maximum occur near the same initial angular momentum as found in Paper I? What is the dependence of the maximum residual spin on the value of the initial spins of the merging BHs? How close is the maximum final spin to the Kerr limit? The answer to the first question is “yes”. The maximum for the residual angular momentum occurs near $J/M_{adm}^2 \approx 1$ for all cases considered. This conclusion is apparent from Fig. 1, where we show the dependence of the spin of the final BH a/M_h as a function of the initial total (orbital plus spin) angular momentum J/M_{adm}^2 at a constant $\theta = 26.565^\circ$. From top to bottom are the cases $S/M^2 = \{0.4, 0.3, 0.2, 0.1, 0.0, -0.1, -0.2, -0.3, -0.4\}$, respectively, where $S/M^2 = (ma_1 + ma_2)/(2m)^2 = (a_1/m + a_2/m)/4$ is the total initial spin of the binary with a_1/m and a_2/m the individual BH dimensionless spin parameters. For reference, in the $S/M^2 = 0.4$ case, we show error bar estimates obtained from Richardson extrapolation.

An interesting feature in the results displayed in Fig. 1 is the crossing of lines for negative S/M^2 . The crossing occurs because the mergers with negative S/M^2 do not suffer the “hangup” of the positive counterparts [2]. Therefore, as S/M^2 becomes more negative, one is able to increase the total angular momentum J/M_{adm}^2 to higher values before reaching the maximum spin a/M_h , which roughly corresponds to the transition between direct plunges and inspiral-like coalescences.

We have looked for but find very little torque-up, suggesting very little spin-orbit coupling. At the same time,

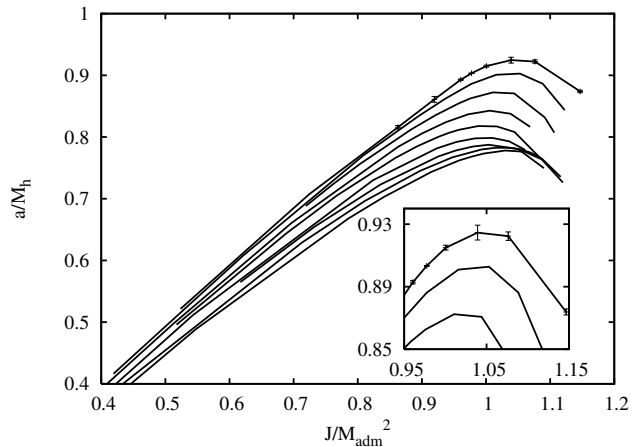


FIG. 1: Final spin a/M_h vs the initial total (orbital plus spin) angular momentum J/M_{adm}^2 at a constant $\theta = 26.565^\circ$. From top to bottom are the cases $S/M^2 = \{0.4, 0.3, 0.2, 0.1, 0.0, -0.1, -0.2, -0.3, -0.4\}$, respectively. As a reference, error bar estimates are given for the $S/M^2 = 0.4$ case.

for the configurations we consider, the final spin as a function of J depends only on the total initial spin, not how it is distributed between the interacting BHs. For instance, the cases $a_{1,2}/m = \{0.4, 0.4\}$ ($S/M^2 = 0.1 + 0.1$), $a_{1,2}/m = \{0.0, 0.8\}$ ($S/M^2 = 0.0 + 0.2$) and $a_{1,2}/m = \{0.6, 0.2\}$ ($S/M^2 = 0.15 + 0.05$), which have the same initial total spin $S/M^2 = 0.2$ but distributed differently between the two BHs, produce almost identical final merged BH angular momentum vs. the initial total angular momentum J/M_{adm}^2 . We have carried out similar experiments for total $S/M^2 = 0.1$ (with $a_{1,2}/m = \{0.8, -0.4\}$ and $a_{1,2}/m = \{0.2, 0.2\}$) and $S/M^2 = 0$ (with $a_{1,2}/m = \{0.0, 0.0\}$, $a_{1,2}/m = \{0.4, -0.4\}$ and $a_{1,2}/m = \{0.8, -0.8\}$). These results suggest that the initial spin is simply “bundled into” the total J in the evolution. A fraction of J is then deposited into the final BH, so that the final BH spin depends essentially only on the *total* initial angular momentum.

This result is confounding because a close examination of the orbits shows significant differences between two cases with the same total but different distribution of initial spin. For instance, the case $a_{1,2}/m = \{0.4, 0.4\}$ with symmetrical initial data yields a significantly different evolution from the case $a_{1,2}/m = \{0.0, 0.8\}$. In fact, the $a_{1,2}/m = \{0.0, 0.8\}$ case produces a *kick* of ~ 175 km/sec, and the symmetric case $a_{1,2}/m = \{0.4, 0.4\}$ produces no kick [4–7].

We argued in Paper I that the existence of the maximum in the final spin parameter a/M_h depends on the participation of an “intermediate excited state” which we characterized as essentially a highly distorted BH. Existence of such an intermediate state seems to be generic, and it emits the largest part of the radiated energy and angular momentum. We conjecture that the non-linearity of such a state will produce such strong radia-

tion of angular momentum that it will enforce an upper limit on the residual BH angular momentum. We extend that argument here to claim that, while in this state, substantial information is lost about the initial configuration of the system.

The answers to the second question (“how does the final BH depend on the initial total spin?”) can be found in Fig. 2 where we show the maximum spin a/M_h deposited in the final BH *vs* the initial total spin angular momentum S/M^2 . From top to bottom are $\theta = \{26.565^\circ, 32^\circ, 45^\circ, 55^\circ, 70^\circ, 80^\circ, 90^\circ\}$, respectively. Each $\theta = \text{constant}$ line in Fig. 2 is obtained from the set of maximum final spins like those found in Fig. 1 for $\theta = 26.565^\circ$. Notice in Fig. 2 that the dependence of the final spin on the spins of the merging BHs is almost linear for θ approaching 90° but non-trivial for small values of θ . The small θ values correspond to small impact parameters. For these cases, mergers with negative S/M^2 are direct plunges; very little angular momentum is radiated, thus the turn around observed in Fig. 2.

A possible answer to the third question (“what is the *maximum* final spin in these mergers?”) can be found by extrapolating the $\theta = \text{constant}$ lines in Fig. 2 to maximally spinning incident BHs (*i.e.* to $S/M^2 = 0.5$). Such extrapolation yields a final BH spin $a/M_h \approx 0.98$. This maximum final spin is slightly lower than the prediction for quasi-circular inspirals by Kesden [8] of $a/M_h \approx 0.9988$ but higher than the estimate by Rezzolla [9] of $a/M_h \approx 0.959$. Recently, work by Sperhake *et al.* [10] has also produced final spins $a/M_h \approx 0.95$ for non-spinning, highly boosted BHs. We believe that these highly boosted BHs address a different regime from the one considered here. The mergers in Sperhake *et al.* [10] involve ultra-relativistic encounters with initial total angular momentum as high as $J/M_{adm}^2 \approx 3$ and small enough impact parameter to “force” a merger; that is, the binaries are initially “over-saturated” with angular momentum. In our case, we start with $J/M_{adm}^2 \approx 1$ configurations and arrange the binary to minimize the radiation losses of angular momentum.

Another important aspect to keep in mind regarding the search for the maximum final spin is that our study involves a 2-parameter family of simulations in S/M^2 and θ . Extrapolation along $\theta = \text{constant}$ as in Fig. 2 may not be the right path in parameter space to find the maximum final spin. To further investigate this point, we plot in Fig. 3 the final spin as a function of θ but now for lines of $S/M^2 = \text{constant}$. From bottom to top are the cases $S/M^2 = 0.0, 0.1, 0.2, 0.3, 0.4$. The crosses along the top axis of the figure are the values obtained from the $\theta = \text{constant}$ extrapolation to extremal BHs in Fig. 2. It is now clear why the maximum final spin values obtained from extrapolating the data in Fig. 2 are similar to each other (*i.e.* all lines approach each other for $S/M^2 = 0.5$). As Fig. 3 shows, the final spin for $\theta \geq 30^\circ$ along $S/M^2 = \text{constant}$ lines is roughly constant thus yielding similar extrapolation values along $\theta = \text{constant}$ (see crosses in Fig. 3).

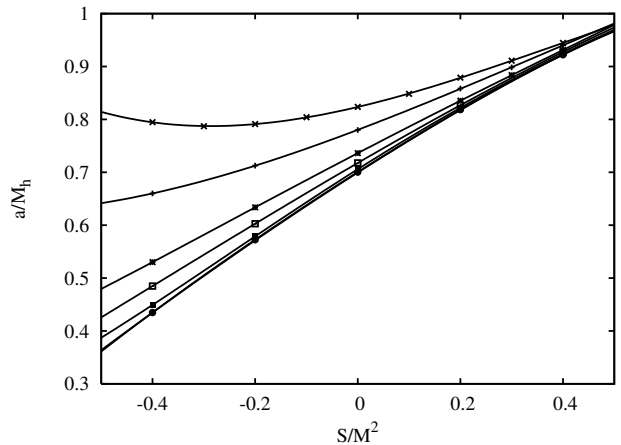


FIG. 2: Maximum final spin *vs* the initial spin angular momentum S/M^2 . From top to bottom are the cases $\theta = \{26.565^\circ, 32^\circ, 45^\circ, 55^\circ, 70^\circ, 80^\circ, 90^\circ\}$, respectively.

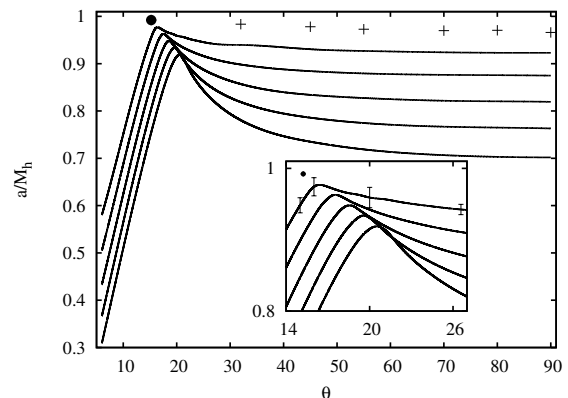


FIG. 3: Maximum final spin *vs* θ for $S/M^2 = 0.0, 0.1, 0.2, 0.3, 0.4$ (bottom to top)

Notice that in Fig. 3 we have extended the range of simulations to include $\theta \leq 26.565^\circ$. A completely different θ dependence is found for these smaller angles, whose details are better appreciated in the inset of Fig. 3, where we have also included the error bars estimates for the $S/M^2 = 0.4$ case. As θ decreases along each $S/M^2 = \text{constant}$ line, the final spin increases and reaches a maximum. Notice in particular from the inset Fig. 3, that the top line, $S/M^2 = 0.4$ case, is not as smooth as the others due to an artificial loss of angular momentum like that seen by Marronetti *et al.* [11]. We however are able to obtain a maximum spin of $a/M_h = 0.98 \pm 0.01$ around $\theta = 16^\circ$. Notice then from Fig. 3 that a better estimate of the maximum (and hopefully global) final spin can be found by an extrapolation to extremal BHs using the values of the maximum on each the $S/M^2 = \text{constant}$ lines in Fig. 3. The result of this extrapolation yields a *maximum final spin* $a/M_h \approx 0.99 \pm 0.01$ at $\theta \approx 15.2^\circ$ and is

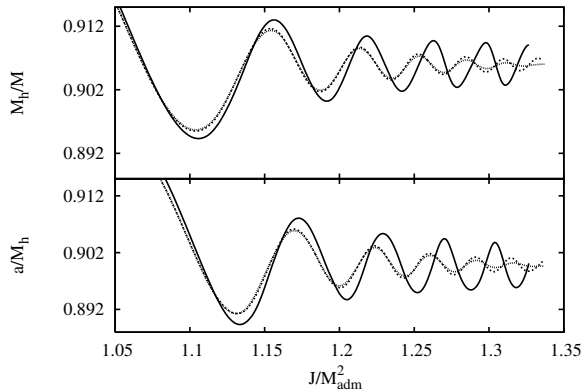


FIG. 4: Final mass M_h/M (top panel) and spin a/M_h (bottom panel) vs J/M_{adm}^2 for $\theta = 60^\circ$ (solid), 80° (dash) and 90° (dotted) with initial total spin of $S/M^2 = 0.4$. The 80° and 90° results almost exactly overlap.

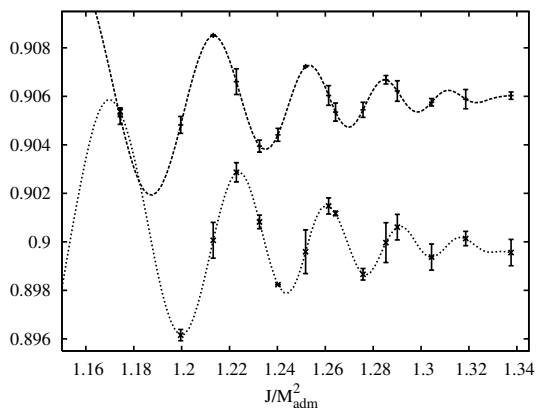


FIG. 5: Final mass M_h/M (dashed, top) and spin a/M_h (dotted, bottom) vs J/M_{adm}^2 with error bars for $\theta = 90^\circ$ and $S/M^2 = 0.4$.

depicted as a black dot in Fig. 3. Also very important to point out is that, although this study involved simulations in the highly non-linear regime of general relativity, the data used to extrapolate to maximum final spin exhibit only a slight departure from linearity (see maximum values in the inset of Fig. 3 and upper right corner data in Fig. 2). In summary, our study consists of a 2-parameter $\{S/M^2, \theta\}$ family of simulations, with global maximum $a/M_h \approx 0.99 \pm 0.01$ of the final spin found by slicing the data along $S/M^2 = \text{constant}$ lines.

Golden Black Hole: In addition to studying the maximum possible final spin, we investigated the final state $\{M_h/M, a/M_h\}$ as one increases the initial angular momentum J/M_{adm}^2 . The results for the case $S/M^2 = 0.4$ with $(a_{1,2}/m = 0.8)$ and angles $\theta = \{60^\circ, 80^\circ, 90^\circ\}$ can be found in Fig. 4. In order to get a sense of the accuracy of our results, we repeat in Fig. 5 the case $\theta = 90^\circ$ and $S/M^2 = 0.4$ including error bar estimates for both

the final mass and spin. It is interesting that as J/M_{adm}^2 is increased, the pair $\{M_h/M, a/M_h\}$ exhibits decaying oscillations around some values $\{\widehat{M}_h/M, \widehat{a}/M_h\}$. After a close examination of the orbits that lead to these results, we concluded that these oscillations are a direct consequence of the binary having to undergo multiple zoom-whirl episodes to shed the “excess” of angular momentum that inhibits the merger [12]. Note also that for a given angle θ , the amplitude of the oscillations are closely similar between a/M_h and M_h/M . The two quantities are 90° out of phase. Furthermore, the frequency of the oscillations is not constant but increases for larger J/M_{adm}^2 .

In order to get a better insight on the oscillation and, in particular, to investigate whether the damping of the oscillations continues for larger J/M_{adm}^2 , we focused our attention on the case $S/M^2 = 0$. Vanishing initial spins not only yield shorter merger times but also require lower resolutions, thus reducing the computational cost of the large number of simulations needed. Figure 6 shows M_h/M (top) and a/M_h (bottom) vs J/M_{adm}^2 for $\theta = 90^\circ$ and non-spinning initial BHs. Crosses are the data from the simulations and solid lines are fits to

$$\frac{a}{M_h} = \frac{\widehat{a}}{M_h} + A_{\pm} e^{\pm B_{\pm} \phi} \sin(\phi) \quad (1)$$

$$\frac{M_h}{M} = \frac{\widehat{M}_h}{M} + D_{\pm} e^{\pm C_{\pm} \phi} \cos(\phi) \quad (2)$$

with ϕ a monotonically growing third order polynomial in J/M_{adm}^2 . The fittings were done as follows: Around $J_*/M_{adm}^2 \approx 0.985$ (vertical line in Fig. 6) the oscillation is almost completely damped out. We have then divided the data into values below and above J_*/M_{adm}^2 . For those below, we fit a decaying exponential and, similarly, a growing exponential for the data above values J_*/M_{adm}^2 . For the fitting, we have ignored the four points in the neighborhood of J_*/M_{adm}^2 since in that region the oscillations are almost completely damped.

An interesting finding is that, modulo a phase shift, ϕ is basically the same fitting function (i.e. similar constant coefficients in the third order polynomial in J/M_{adm}^2) for the decaying and growing sectors. We also obtain that both the decaying and growing fittings yield the same values of $\{\widehat{M}_h/M, \widehat{a}/M_h\} = \{0.951, 0.685\}$. The only changes are in the constants $\{A_{\pm}, B_{\pm}, C_{\pm}, D_{\pm}\}$. Finally, the exponential envelopes (dashed lines in Fig. 6) cross approximately at J_*/M_{adm}^2 . For this non-spinning situation, we repeated similar analysis for $\theta = 70^\circ$ and found the same values for $\{\widehat{M}_h/M, \widehat{a}/M_h\}$ within our numerical errors. In addition, we considered total initial spins cases $S/M^2 = 0.2$ ($\theta = 90^\circ$) and $S/M^2 = 0.4$ ($\theta = 60^\circ, 80^\circ, 90^\circ$). The $S/M^2 = 0.2$ case yielded $\{\widehat{M}_h/M, \widehat{a}/M_h\} = \{0.936, 0.800\}$, and the $S/M^2 = 0.4$ values $\{\widehat{M}_h/M, \widehat{a}/M_h\} = \{0.906 \pm 0.001, 0.900 \pm 0.001\}$, with the last case selected for error estimates. We name the BHs with parameters $\{\widehat{M}_h/M, \widehat{a}/M_h\}$ the *golden* BHs.

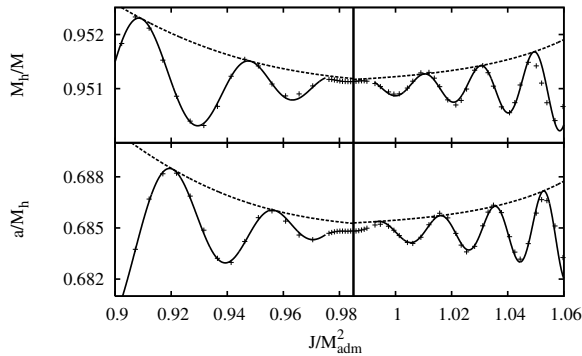


FIG. 6: M_h/M (top) and a/M_h (bottom) vs J/M_{adm}^2 for $\theta = 90^\circ$ with initial total spin of $S/M^2 = 0.0$.

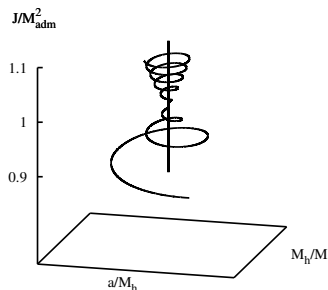


FIG. 7: Final spin a/M_h vs final mass M_h/M vs J/M_{adm}^2 for 90° with initial total spin of $S/M^2 = 0.0$.

Figure 7 combines the results from Fig. 6. The vertical line denotes the location of the *golden* BH. The result is a logarithmic spiral which approaches the *golden* BH as J/M_{adm}^2 nears $J_*/M_{adm}^2 \approx 0.985$ from above or below. A similar spiral is found in the a/M_h vs M_h/M plane when the angular momentum J/M_{adm}^2 is held constant and one plots them instead as a function of the angle θ . The center of the spiral is again at the *golden* BH. A closer look at our simulations reveals the identity of the *golden* BH as the final BH obtained from the merger of a binary of the corresponding spinning BHs in a quasi-circular inspiral. We are currently investigating the reasons behind this finding.

Conclusions: From the first studies of binary BH mergers [13–15], it became apparent that merger waveforms have a simpler structure than was expected. Here we have presented two more examples of reduction of complexity. One is the invariance of the final BH spin vs the initial total angular momentum with respect to how the individual spins are distributed between the interacting BHs. The other invariance is the final $\{\widehat{M}_h/M, \widehat{a}/M_h\}$ of the *golden* BH with respect to the angle θ , for a given total initial spin S/M^2 (see Fig. 4). These are explicit reductions of degrees of freedom from the initial data to the final BH. From the results of our 2-parameter family of simulations, we estimated that the maximum final spin is found for initial extremal BHs with spins aligned with the orbital angular momentum and $\theta \approx 15.2^\circ$. Our results imply a maximum final spin $a/M_h \approx 0.99 \pm 0.01$.

This work was supported in part by NSF grants PHY-0653443 (DS), PHY-0914553 (PL), and PHY-0855892 (PL,DS). Computations carried out under LRAC allocation MCA08X009 (PL,DS) and at the Texas Advanced Computation Center, University of Texas at Austin. We thank Y. Chen, M. Kesden and U. Sperhake for their comments and suggestions.

-
- [1] M. C. Washik, J. Healy, F. Herrmann, I. Hinder, D. M. Shoemaker, P. Laguna, and R. A. Matzner, Phys. Rev. Lett. **101**, 061102 (2008), 0802.2520.
 - [2] M. Campanelli, C. O. Lousto, and Y. Zlochower, Phys. Rev. D **74**, 041501 (2006), arXiv:gr-qc/0604012.
 - [3] F. Pretorius and D. Khurana, Classical and Quantum Gravity **24**, 83 (2007), arXiv:gr-qc/0702084.
 - [4] F. Herrmann, I. Hinder, D. M. Shoemaker, P. Laguna, and R. A. Matzner, Phys. Rev. D **76**, 084032 (2007), 0706.2541.
 - [5] F. Herrmann, I. Hinder, D. Shoemaker, P. Laguna, and R. A. Matzner, Aptrophys J. **661**, 430 (2007).
 - [6] M. Koppitz et al., Phys. Rev. Lett. **99**, 041102 (2007), gr-qc/0701163.
 - [7] L. Rezzolla, E. N. Dorband, C. Reisswig, P. Diener, D. Pollney, E. Schnetter, and B. Szilágyi, Astrophys. J. **679**, 1422 (2008), 0708.3999.
 - [8] M. Kesden, Phys. Rev. D **78**, 084030 (2008), 0807.3043.
 - [9] L. Rezzolla, Classical and Quantum Gravity **26**, 094023 (2009), 0812.2325.
 - [10] U. Sperhake et al., Phys. Rev. Lett. **103**, 131102 (2009), 0907.1252.
 - [11] P. Marronetti, W. Tichy, B. Bruegmann, J. Gonzalez, and U. Sperhake, Phys. Rev. **D77**, 064010 (2008), 0709.2160.
 - [12] J. Healy, J. Levin, and D. Shoemaker, Phys. Rev. Lett. **103**, 131101 (2009), 0907.0671.
 - [13] F. Pretorius, Phys. Rev. Lett. **95**, 121101 (2005), gr-qc/0507014.
 - [14] J. G. Baker, J. Centrella, D.-I. Choi, M. Koppitz, and J. van Meter, Phys. Rev. Lett. **96**, 111102 (2006), arXiv:gr-qc/0511103.
 - [15] M. Campanelli, C. O. Lousto, P. Marronetti, and Y. Zlochower, Physical Review Letters **96**, 111101 (2006), arXiv:gr-qc/0511048.